EFSUMB Course Book, 2nd Edition

Editor: Christoph F. Dietrich

Ultrasound of the chest

Gebhard Mathis[1], Annia Schreiber[2], Zeno Spârchez[3], Giovanni Volpicelli[4]

[1]Praxis for Internal Medicine, Rankweil, Austria.

[2]Division of Respirology, Department of Medicine, University Health Network, Toronto, Canada.

[3]Institute for Gastroenterology and Hepatology, Department of Ultrasound. "Iuliu Hatieganu", University of Medicine and Pharmacy, Cluj-Napoca, Romania.

[4]Department of Emergency Medicine, San Luigi Gonzaga University Hospital, Torino, Italy.

Corresponding author:

Gebhard Mathis, MD., FCCP.

Praxis for Internal Medicine, Rankweil, Austria

Email: gebhard.mathis@cable.vol.at

Technical requirements

Sonographic examination of the chest wall and axillary/supraclavicular region generally requires a linear array probe using frequencies between 5 to 10 MHz. For pleural and peripheral pulmonary lesions, sector scanners are more suitable for intercostal access to the pleura and lung through the narrow intercostal spaces. Tilting and angulation of the probe provides a good view of most parts of the pleura and of underlying pulmonary consolidation. Convex arrays provide better images and give a greater field of view when the examiner subtracts the rib shadows from the picture. For sonographic examination of the pleura and lung, frequencies between 3.5-15 MHz are recommended. For daily clinical use in chest sonography, the best combination of probes is a 3.5-5 MHz sector or curved array probe and a small parts linear scanner with a frequency of 5-12 MHz (15 MHz, if necessary). This combination is used in many other settings, e.g. abdominal, vascular and small parts ultrasound [(1)].

Examination technique

Chest sonography is a point of care ultrasound. Thus, the examination is tailored to the patient's symptoms, e.g. pain or dyspnoea. The position in which the patient is scanned depends on the clinical question. In a systematic examination, usually the dorsal and lateral images are obtained with the patient sitting, whereas the supine position is used for visualising the ventral side. Raising the arms and crossing them behind the head causes the intercostal spaces to be extended and facilitates access. The examiner is able to visualise the region behind the shoulder blade if the patient puts their hand on the contralateral shoulder. The transducer is moved along the intercostal space in a dorsal to ventral direction in both longitudinal and transverse planes. Rotating the probe in different positions provides the examiner with a three-dimensional image. During every stage of the examination, the user should determine the movement of the pleura in relation to respiration, the so-called sliding sign [Figures 1 and 2].

Figure 1 **Linear probe placed intercostally in an oblique view (a). The right arm is elevated behind the head or positioned on the contralateral shoulder. The intercostal spaces are extended and the scapula is turned. Corresponding sonographic view with the sliding line of the visceral pleura (b).**

a

b

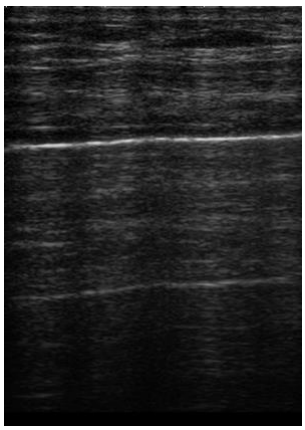

Figure 2 Linear probe in an anterior longitudinal scan (a). Corresponding sonographic image, the sliding line of the visceral pleura can be seen (b) below the cartilage (C) of the ribs (R).

a

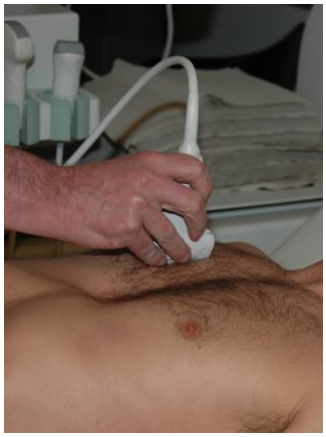

b

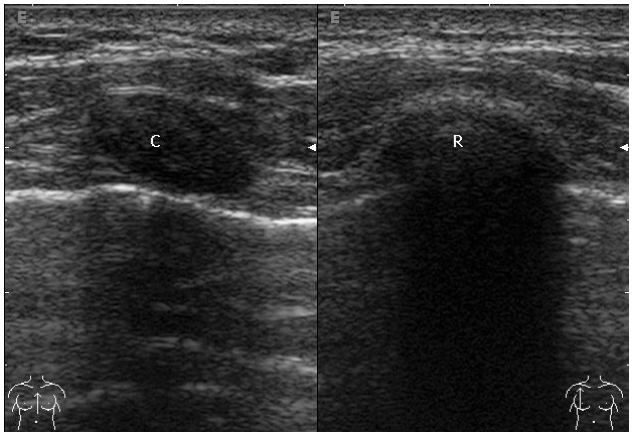

The diaphragm is examined through the subcostal section of the abdomen via the transhepatic route on the right and to a lesser extent through the spleen on the left [Figure 3]. The axilla should be examined in the supine position with the arm abducted over the head. Supraclavicular access allows the investigator to view the region of the brachial plexus, the subclavian vessels and the lung apex. From a suprasternal approach, the anterior upper mediastinum can be viewed. Immobile and intensive care patients are examined by turning them to the oblique position in the bed [(1)].

Figure 3 **Transhepatic examination. Convex probe placed subcostally from the right (a). Corresponding sonographic image, lung is indicated by a mirror artefact above the diaphragm (D) (b).**

a

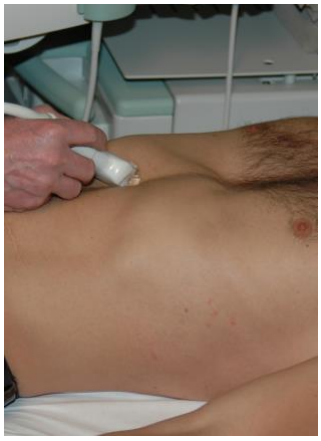

b

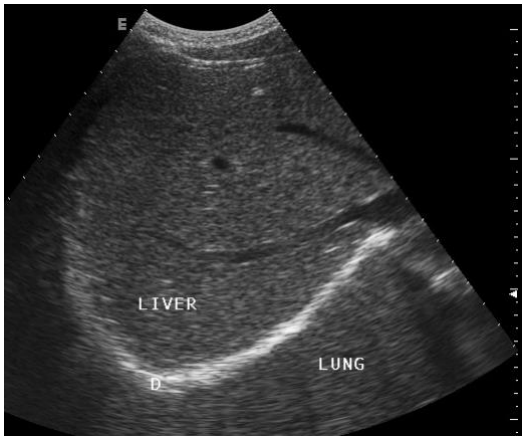

Figure 4 **Examination of the supraclavicular region. Linear probe placed longitudinally on the lateral base of the neck (a). Corresponding sonographic image (b). Brachial plexus (N); Scalene muscles (M).**

a

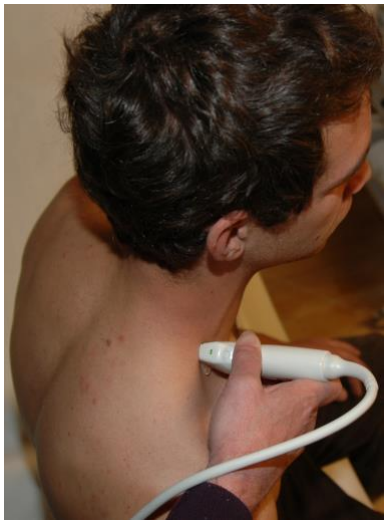

b

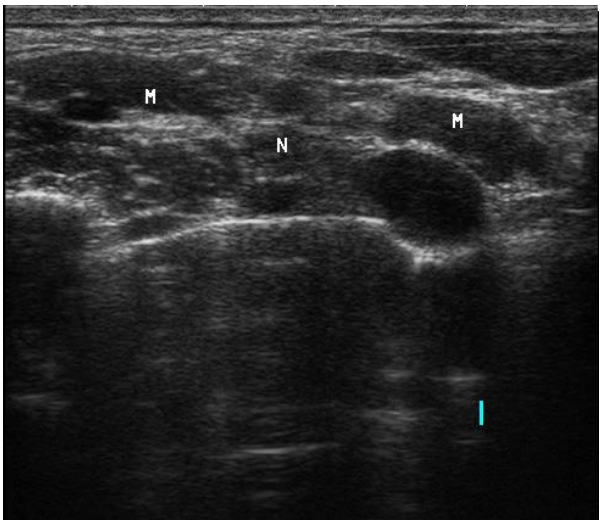

Chest Wall

Soft tissue lesions

Suspicious or unclear findings during palpation of the chest wall should be initially examined by ultrasound. In most cases the examiner will find lymph nodes, which are the most

clinically relevant finding. However, haematomas and lipomas are also visualised by ultrasound. Haematomas are echo-free or hypoechoic and show blurred internal echoes. The echogenicity of haematomas depends on the amount of extravasated blood and the stage of organisation. Lipomas have a similar but largely hypoechoic ultrasound picture. Their echogenicity depends on the fat content of cells [Figure 5]. In cases of painful swelling in the region of the axilla, a sweat gland abscess can be differentiated from a lymph node.

Figure 5 Palpable mass on the back. An oval encapsulated lesion is visualised, a typical lipoma.

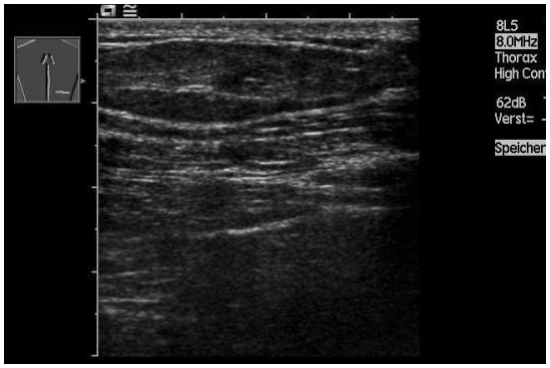

Lymph nodes

Reactive and inflammatory lymph nodes are a very common finding in the axilla and supraclavicular fossa. On ultrasound, their typical shape is oval or triangular, some are long and thin [Figure 6]. The so-called hilum fat sign is found in the centre of reactive lymph nodes. This echogenic centre becomes larger during the healing process of inflammatory lymph nodes.

Malignant lymphomas also appear echolucent. They are rounded, sharply bordered and expansive, but in most cases they are non-infiltrating. Although some sonomorphological criteria exist to help distinguish the aetiology of lymph nodes, they may have similar appearances despite having different origins. If immediate treatment is required, ultrasound guided needle biopsy may help to make a swift diagnosis. Alternatively, regular follow up scans may provide reassurance depending on the clinical course.

The diagnosis or exclusion of lymphatic metastatic disease is a question frequently raised by clinicians. Lymph node metastases appear as round to oval, inhomogeneous structures with irregular margins and irregular vascularisation [Figure 7]. However, they typically show extracapsular growth into irregular borders and diffuse infiltrating growth into vessels and the surrounding tissue. Necrosis, calcification or partial lymph node infiltration may produce an inhomogeneous ultrasound pattern.

Routine ultrasound evaluation of supraclavicular lymph nodes reveals suspicious lymph nodes in a high number of patients with lung cancer. High-resolution ultrasound is superior to CT in the detection of pathological lymph nodes, especially of non-palpable lymph nodes. Ultrasound guided biopsy can prove malignancy and thereby a N3 or M1 stage. Thus, more invasive and expensive procedures can be avoided. Non-palpable lymph nodes and metastatic disease in reactive lymph nodes can be detected [(2)].

Figure 6 **Painful swelling in the right axilla. Differential diagnoses are lymph node or abscess of a sweat gland. Echo-poor solid structure with a 'hilum sign' (a). A reactive inflammatory lymph node with regular vascularisation (b).**

a

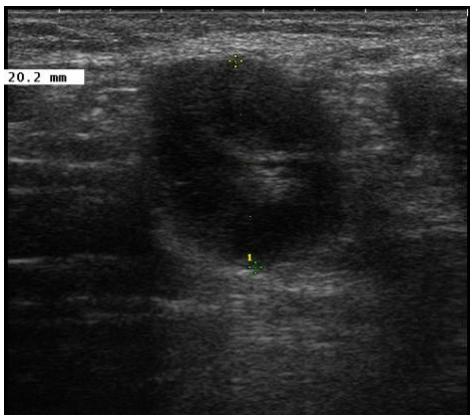

b

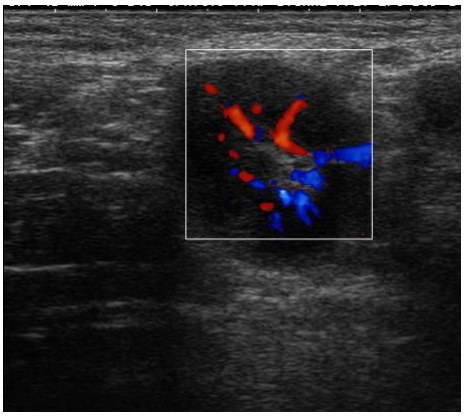

Figure 7 Neck lymph node metastasis of an epidermoid lung cancer (a). Ultrasound guided fine needle aspiration biopsy of a supraclavicular lymph node (b), the needle is shown.

a

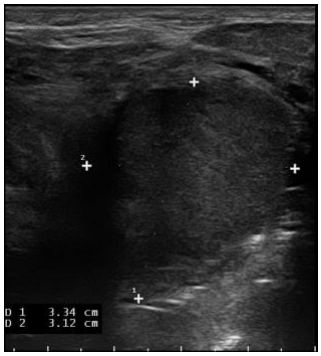

b

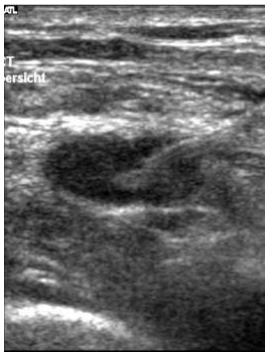

Bony lesions

On chest X-ray, non-displaced rib fractures are frequently not seen. It may seem surprising at first glance that the diagnosis of rib fractures is made twice as frequently by sonography compared to chest radiography. Typical sonographic findings of rib fractures are gaps, steps, dislocations, haematomas and minimal concomitant pleural effusions, pneumothoraces and lung contusions [Figure 8 and 9]. Very small dislocations and fissures are detected by the presence of reverberation artefact at the point of trauma, also known as the so-called chimney phenomenon [(3, 4)]. When performing the ultrasound examination, the patient indicates the site of pain and the examiner obtains a cross-sectional image of the region in two planes, with the image closely following the course of the ribs.

Osteolytic metastases in the bony thorax cause disruption of the cortical reflex with pathological ultrasound transmission. Osteolytic lesions are usually seen as well-demarcated, round or oval, space-occupying lesions with a partly hypoechoic and partly rough structure. Colour-coded duplex sonography reveals corkscrew-like neovascularisation or a vascular inferno, especially in patients with multiple myeloma [Figure 10].

When diagnosing chest wall infiltration in cases of lung cancer, ultrasound is significantly superior to CT. Direct evidence of infiltration of wall structures and rib destruction are reliable diagnostic criteria. An interruption of the pleural reflex and/or limited respiratory motion of the space-occupying lesion provides an indication but not proof of infiltration of the chest wall. Accompanying inflammatory reactions can also be an indicative of chest wall infiltration [(5)].

Figure 8 Rib fracture. Tiny (1 mm) fracture line of the corticalis.

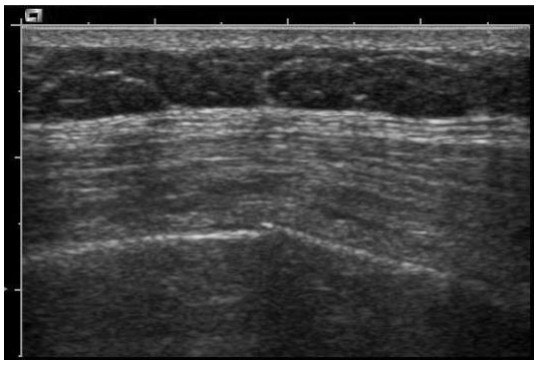

Figure 9 Sternal fracture caused by a car accident. A 6 mm step (++) is seen.

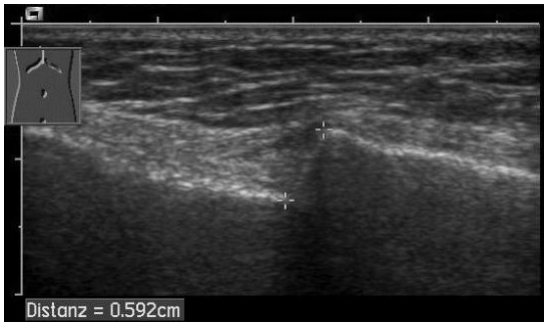

Figure 10 Multiple myeloma in a palpable thickened rib with irregular vascularisation. The final diagnosis was established by ultrasound guided biopsy.

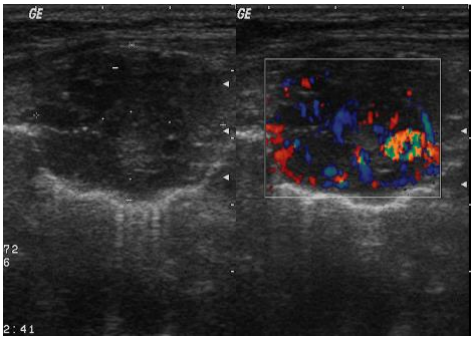

Pleural diseases

Introduction

The pleura is a thoracic structure which can be easily examined by ultrasound. With an appropriate technique, the entire costal and diaphragmatic pleura may be visualised. This is of great importance since most diseases of the pleura affect those pleural segments.

Normal sonographic appearance

The pleural space is superficial and can be easily examined by ultrasound using either a direct intercostal or an abdominal approach.

The use of high frequency 5-17 MHz linear probes applied directly to an intercostal space provides excellent visualisation of the pleural space. The pleural space is located within 1 cm of the rib interface. The normal pleura has a thickness of only 0.2-0.4 mm and may be difficult to detect even with the latest ultrasound equipment.

The visceral pleura appears as a fine echogenic line which is normally included within the thick line of total reflection of ultrasound waves at the air-filled lung. The bright, linear interface produced by the air-filled lung covered by visceral pleura moves backwards and forwards with respiration, this is known as the ‘gliding sign’. Small, uneven irregularities at the visceral pleural surface produce reverberations named ‘comet tail’ artefacts. Such

artefacts, rarely seen in the normal lung, are most frequently demonstrated in cases of interstitial lung disease or when the pleural space is scanned through a normal liver [(1, 6, 7)].

The pleural cavity has an echo-free to hypoechoic appearance due to the presence of a small amount of fluid. The parietal pleura appears as a fine, sometimes weakly echogenic line, often obscured by reverberation artefacts [Figure 11]. With high resolution transducers, the line of parietal pleura may be divided into 2 layers: the parietal pleura and the external endothoracic fascia [(1, 6, 7)]. Sometimes the parietal pleura is accompanied by a thin hypoechoic layer and nodular hypoechoic spreading which represents the extrapleural lamella of fat [(1, 6)]. The visceral pleura is more difficult to visualise in normal lung as it is embedded in the near total reflection of ultrasound waves over the air-filled lung [(6)]. In cases of consolidation, the visceral pleura appears as an echogenic line [(1)].

Figure 11 Pleura. Normal sonographic appearance. Very thin echogenic line corresponding to parietal pleura and the endothoracic fascia. Echo-poor pleural space. Strong total reflexion from the aerated lung, the so-called visceral pleura.

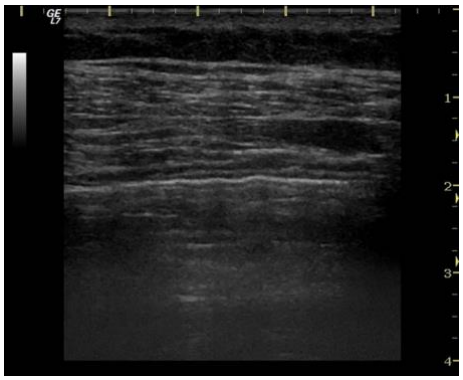

When scanned using an abdominal approach, the diaphragm shows a bright, curving echogenic line that moves with respiration. When the lung above the diaphragm is filled with air, the curved surface of the diaphragm lung interface acts as a specular reflector and produces a mirror image of the liver or spleen above the diaphragm [(7)].

Pleural effusion

Signs of pleural fluid

A pleural effusion was the first pathological entity visualised by ultrasound. In abdominal ultrasonography both the right and left diaphragmatic pleura can be imaged through the liver or spleen and pleural fluid may be depicted in those areas.

The sonographic hallmark of pleural fluid is an echo-free zone between the parietal and visceral pleura. This may be detected through both intercostal (better) or abdominal approaches. The use of a direct intercostal approach with high resolution linear array transducers allows the detection of even minute amounts of pleural fluid. Other signs of pleural effusion are described in Table 1.

Table 1 Sonographic signs of pleural fluid

1. Echo-free zone separating the visceral and parietal pleura
2. Echo-free zone displaying a change of shape during respiration
3. Floating and moving echogenic particles
4. Moving septations within the pleural space
5. Moving lung within the fluid
6. 'Fluid colour' sign on Doppler sonography

The diagnosis of large and medium pleural effusions is easily made by ultrasonography [Figure 12]. However, small amounts of fluid, especially when located between the chest wall and diaphragm or in the vicinity of hypoechoic pleural thickening are detected with great difficulty [(6, 7)]. In such cases, the use of the above mentioned criteria [(1, 7-10)] may be very helpful. The 'fluid colour' sign is a colour signal detected by Doppler sonography that appears within a fluid collection in the pleural space during respiratory or cardiac cycles [(1)]. It has a high sensitivity (89.2%) and specificity (100%) for detecting minimal or loculated effusions [(1)]. Pleural effusions located in the interlobular spaces are usually not visible on ultrasound [(7)].

Figure 12 Large, echo-free pleural effusion. Note the presence of artefacts and a needle for thoracocentesis.

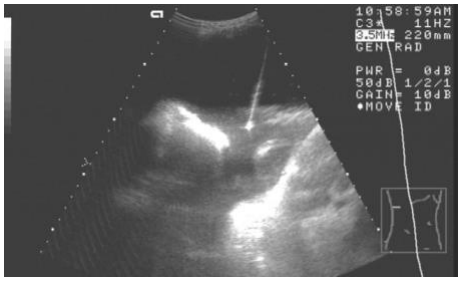

Detection limit and volume estimation

Very small volumes of pleural fluid (as little as 5 ml) can be identified sonographically in the angle between the chest wall and diaphragm in patients in standing or sitting positions. For a standard X-ray in the same setting, the detection limit is 150ml [(6)]. Moreover, the standard X-ray has a low detection rate in patients lying in bed or in effusions accompanied by atelectasis [(6)].

Due to anatomical differences, various shapes of the thorax and respiration related changes, an exact measurement of the volume of the effusion is not possible with any imaging modality. However, a reliable estimation is very desirable in clinical practice to help guide further management including the need for a therapeutic puncture and to ensure appropriate follow up.

There are several methods that can be used to measure the volume of pleural effusions by means of sonography. The best accuracy is achieved by planimetric measurements of the square dimensions of effusions in various longitudinal and transversal sections.

For sitting patients a good method is to multiply the lateral height of the effusion in cm by 90 [(6)]. In supine patients the measurement of the volume is made using the formula 50x-800, where x is the thickness of the dorsal fluid layer in millimetres measured at a right angle to the chest wall [(6)]. Using both these methods, an estimation of pleural fluid volume in mL will be obtained

In routine clinical settings, a rough estimation of the effusion volume (small, medium, large) by measurement of the longitudinal and transverse diameters is usually sufficient and the results are reproducible and operator independent [(7)].

Types of effusion

Establishing the type of effusion is important in order to determine the underlying diagnosis. Transudates do not contain any components within the fluid and are thus echo-free. Exudates contain cells, protein, fibrin or blood and are often echogenic, sometimes with septations or fibrin strands inside. Echoes float or swirl in the liquid and can be easily differentiated from artefacts [(6, 7)]. The additional findings of pleural nodules or thickening always indicate an exudate. A further classification of pleural effusions into anechoic, complex non-septated, complex septated and homogeneously echogenic may be helpful in some cases [(8)].

In prospective studies it has been demonstrated that transudates are either anechoic (45%) or complex non-septated (55%) whereas exudates may be echo-free or echogenic [(1, 6, 7, 9)]. A definitive diagnosis is made by thoracocentesis and pleural fluid analysis. Malignant effusions are more often echogenic than echo-free and are accompanied by pleural thickening and/or solid nodular structures [(1)]. The presence of pleural/diaphragmatic nodules, a pleural/diaphragmatic thickness >10 mm and a swirling sign is strongly associated with malignant effusions [(10)]. The lung air bronchogram sign and a complex septated ultrasound pattern are more common in benign pleural effusion [(10)]. A diffuse, regular pleural thickening with echogenic septa (a complex septated pattern) signifies pleural inflammation.

Complicated pleural effusions

Infected parapneumonic effusions, septated or loculated pleural effusions are described as complicated effusions. Ultrasonography is a very good method for visualising septations but cannot diagnose infection which is proven only by pleural fluid aspiration and analysis [Figure 13].

A parapneumonic effusion is an exudative effusion associated with pneumonia (in approximately 40% of cases) or a lung abscess. In addition to the ultrasound signs of

pneumonia, a small amount of fluid is seen in the pleural space and the visceral pleura is thickened and hypoechoic demonstrating signs of inflammation.

In empyema there is frank pus with bacteria or other infectious organisms in the pleural space. The main causes of empyema are infections from pneumonia, trauma, surgery, thoracocentesis and oesophageal rupture. Three stages of empyema have been described: exudative, fibrinopurulent and organised. In the exudative stage, multiloculated effusions with large floating echoes with different echogenicity of the contents may be seen [Figure 13]. The fibrinopurulent stage is characterised by fibrin deposition on the pleura which is moderately thickened in a capsule-like fashion. The fluid may be loculated with limited membrane formation. In the final organised stage, a rigid membrane around the lung called pleural peel is produced [(1, 7)]. Empyema should be differentiated from a subpleural lung abscess.

Figure 13 Echogenic pleural effusion in a patient with metastatic pleural disease.

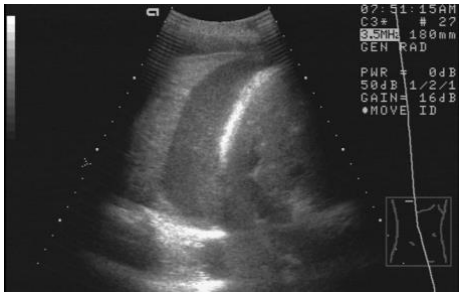

Haemothoraces are seen in patients with underlying lung or pleural malignancy or after chest trauma. The ultrasound signs vary depending on the time from the trauma. A collection of fresh blood may be echo-poor whereas older collections are echogenic, with both fine echoes and large echogenic structures representing clots [Figure 14] [(6)]. The sensitivity of ultrasound in detecting a haemothorax after trauma is equivalent to that of chest radiography, but ultrasound is a much faster procedure [(7)]. Chylothorax, often linked with thoracic malignancies, is also variably echogenic owing to the reflections occurring at lipid aggregates [(7)].

Figure 14 Septated pleural fluid in a patient with an infected effusion.

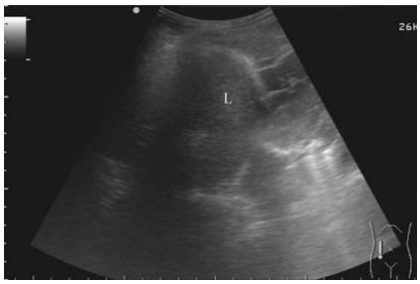

Solid pleural lesions

The solid pleural changes encountered in clinical practice are listed in Table 2.

Table 2 Solid pleural lesions.

Diffuse pleural thickening (due to fibrosis and/or infiltration)

- fibrothorax, pleural peel, pachypleuritis
- malignancy

Focal pleural thickening (due to inflammation and/or fibrosis)

- pleuritis (inflammation)
- pleural plaque (fibrosis)

Pleural masses

- benign pleural tumours
- pleural metastases
- pleural mesothelioma
- transpleural growth of tumours

Acute or chronic pleural inflammation may be easily demonstrated by ultrasound. The ultrasound findings are (a) hypoechogenic thickening of pleura often with a rough appearance and interruption of the normally smooth pleura, (b) small subpleural consolidations between 2-20 mm in size, round or wedge shaped, (c) localised pleural

effusions and (d) fibrinous echogenic bands at the lung surface, towards the parietal pleura or dividing an accompanying pleural effusion [(1, 6, 7, 11)]. The presence of a large pleural effusion with echogenic septations/strands and subpleural infiltrates favours the diagnosis of tuberculosis [Figures 15] [(6)].

Figure 15 Localised pleural thickening in a patient with post inflammatory pleural fibrosis.

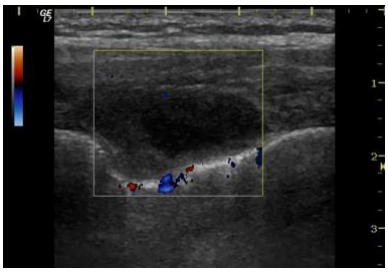

Pleural fibrosis has different echogenicities. It is usually hypoechoic, but older fibrosis tends to be more echogenic. A recently developed fibrosis may be very hypoechogenic and can sometimes be misinterpreted as an effusion. In such cases the use of the 'colour-Doppler' sign may be helpful in establishing the diagnosis. Calcifications are sometimes present in the thickened pleura, most commonly in tuberculosis or empyemas [(1, 6, 7)]. As all these sonographic features are also seen in pleural carcinoma and mesothelioma and sonographic differentiation between them is rarely possible.

Diffuse pleural thickening

Diffuse pleural thickening is a sign of fibrosis or malignancy. It involves the visceral pleura and results in lung entrapment and causes restriction of ventilation. The main causes are exudative pleural effusion, asbestosis related effusion, haemothorax or empyema [(1, 6, 7)]. The diffuse pleural fibrosis observed in malignancy is mainly lobulated, sometimes with multiple discrete pleural masses. Circumscribed (focal) pleural thickening is indicative of inflammation (pleuritis), pleural plaque formation (fibrosis, asbestosis) or malignant infiltration [(1, 6, 7)].

Pleural plaques are found in pneumonia, asbestos exposure, pulmonary infarction, trauma, chemical pleurodesis and drug-induced pleural disease. The ultrasound sign of a pleural plaque is a smooth, elliptical, hypoechoic pleural thickening sometimes with calcifications. The plaque displaces the lung from the chest wall, is well demarcated against the aerated lung and does not infiltrate the chest wall (1-3). In asbestosis the pleural plaques are located mainly in the dorsolateral portion of the costal region of the parietal pleura and contain calcifications in 10% of cases [(1, 6, 7, 11)].

Pleural tumours

Benign pleural tumours

Benign pleural tumours (fibrolipomas, chondromas, neurinomas and benign pleural mesotheliomas) are rare, accounting for less than 5% of pleural tumours. They are round, well demarcated, encapsulated (usually by a fine capsule), hypoechoic or moderately echogenic lesions in the pleural space [Figure 16]. Depending on their size they can displace the surrounding structures but do not invade them. Additional findings are small effusions around the tumour and calcifications [(1, 6, 7, 11)]. Tumours of the peripheral nerves (neurofibroma, schwannoma) located extrapleurally may sometimes mimic a pleural tumour [(11)].

Figure 16 Benign, well demarcated pleural tumour. Histology showed a fibrous solitary pleural tumour.

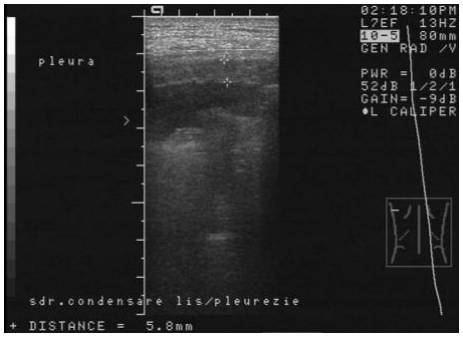

Malignant pleural lesions

Malignant pleural lesions include pleural metastases, pleural mesothelioma, pleural infiltration of bronchogenic carcinoma and pleural lymphoma (very infrequent). Pleural metastases are most commonly found in bronchogenic carcinoma. Primary neoplasms of the breast, gastrointestinal tract, kidneys and ovaries may also metastasise to pleura [(7, 11)]. Their occurrence and visibility are closely related to pleural effusions and they are usually overlooked by sonography due to their small size (<5 mm). High-definition ultrasound equipment and a thorough and systematic examination are mandatory to detect small (< 5 mm) lesions [(7)]. If metastases grow larger, they become more visible on the parietal and diaphragmatic pleura. The metastatic nodules are hypoechogenic to moderately hyperechogenic, may be round or polypoid, sometimes with a broad base. The lesions are well-demarcated against the surrounding tissue or pleural fluid with obtuse margins with the chest wall [(1, 6, 7, 11)]. Large metastases may invade the lung or the chest wall, the invasion being recognised on ultrasound as interrupted or absent delimitation between the lesion and the surrounding tissue.

The combination of a pleural effusion and nodules or sheet like pleural thickening in a patient with a known malignancy is very suggestive of metastatic disease [Figure 17] [(1, 6, 7, 11)].

Figure 17 Pleural metastases from lung cancer.

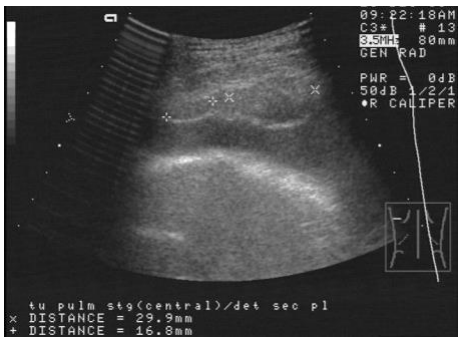

Pleural mesothelioma is a rare, fatal pleural tumour, usually associated with asbestos exposure. The sonographic signs of mesothelioma are (a) diffuse pleural thickening, often

nodular and irregular, (b) calcifications in the pleura, (c) pleural effusion and (d) focal hypo- or isoechoic, vascularised pleural masses [Figure 18] [(7)]. It is a very aggressive tumour that invades the chest wall or diaphragm and spreads to the contralateral pleura or pericardium. The invasion of the chest wall appears as striped, hypoechoic ramifications [(6)].

Figure 18 Malignant mesothelioma. Large pleural tumour invading the lung.

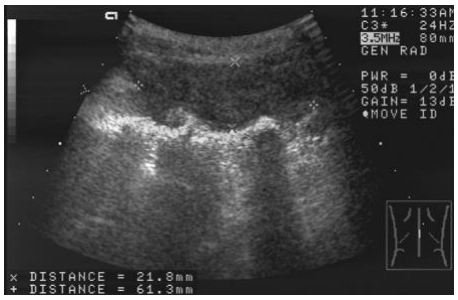

Pleural involvement from bronchogenic carcinoma typically appears as a hypoechoic mass with acute angulation between the lesion and the chest wall [(11)]. If the tumour has infiltrated the parietal pleura it becomes immobile during respiration [(11)]. The main diagnostic challenges in pleural tumours are (a) to ascertain if a single pleural lesion is a metastatic nodule, a benign tumour or a primary pleural tumour, (b) to differentiate between a metastasis located on the visceral pleura and a subpleural pulmonary tumour and (c) to differentiate an extensive or sheet-like infiltration of the pleura in metastatic carcinomatosis from an inflammatory thickening or a tapestry-like mesothelioma [(6)]. These clinical questions can be answered with a needle biopsy.

Interventions in the pleural space

Materials and techniques

The transducers used in ultrasound guided chest interventions in the pleural space vary according to the distance to the target lesion. High frequency linear probes are generally used. In cases of larger pleural masses 3.5 MHz convex transducers may be needed. Due to the presence of narrow spaces between the ribs, small (micro) convex probes are chosen.

Ultrasound offers a number of advantages over other imaging methods (CT or fluoroscopy): (a) the ability to continuously monitor the interventional procedure; (b) the possibility to perform the procedure with the patient in an upright position (providing optimal access to gravity-layered pleural fluid) and even in sick dyspnoeic patients; (c) its multiplanar capability which permits even oblique, angled approaches which are useful in cases of 'difficultly' located thoracic lesions; (d) shorter procedure time (up to 42%); (e) portability; (f) lower cost [(6, 7, 11-15)]. Needle and catheter placement can be monitored under direct and constant sonographic visualisation, ensuring maximum safety and benefit [(6, 12-16)].

Diagnostic thoracocentesis

Ultrasound guided thoracocentesis should be done whenever clinically guided thoracocentesis is unsuccessful or judged to be difficult. An ultrasound scan is performed to confirm the presence of fluid and to select and mark the puncture site. Usually after choosing the puncture site with ultrasound, the probe is removed and the puncture made with careful attention paid to the depth of the collection and the location and depth of the lung. If the fluid collection is small, the puncture and aspiration can be done under continuous ultrasound monitoring. A 22 G needle attached to a 10 ml syringe is generally used for diagnostic aspiration. Occasionally, the pleural fluid may be too viscous to aspirate through a 22 G needle. In such cases, after rechecking the position of the needle, aspiration with a larger needle (20 or 18 G) should be attempted [(1, 14)]. Ultrasound guidance adds accuracy and safety to the procedure, the incidence of pneumothorax drops from 8.89% for clinically guided thoracocentesis to 0.97% with ultrasound guidance [(17)].

Pleural biopsy

Biopsy of pleural masses can be performed using standard biopsy needles (16-20 G). Fine needle aspiration has less value in the diagnosis of pleural tumours, especially for primary pleural tumours such as mesothelioma [(18)]. For non-mesothelial malignancy, the sensitivity of fine needle aspiration (FNA) for malignancy is higher (up to 78%) but typing by means of cytology is seldomly possible [(18)]. Core biopsy using 14-18 G cutting needles is more accurate than FNA in the diagnosis of both focal pleural tumours and diffuse pleural thickening [(18)]. The overall sensitivity in diagnosing pleural malignancy varies between 61-

94% and the accuracy between 62.9-94% [(18, 19)]. Pleural thickness (>3 mm) and the size of the biopsy needle (16 G) are significantly correlated with the diagnostic yield [(19)]. In the detection of pleural mesothelioma sensitivity and specificity are 86% and 100% respectively [(20)]. The presence of a pleural effusion does not significantly influence the sensitivity of core biopsy (88% for malignancy, 93% for pleural mesothelioma) but reduces the risk of complications [(18)].

A wide variety of complications can occur after pleural biopsy including vasovagal reactions, chest wall haematoma, subcutaneous emphysema, infection, haemothorax, air embolism, lung laceration and injury to the liver, spleen and stomach [(14, 15, 18)]. The complication rate of ultrasound guided pleural biopsy varies between 2–5% and is decreased in the presence of a pleural effusion [(18)]. The most encountered complication is pneumothorax with a reported frequency in published series between 0% and 9% [(18)]. Most pneumothoraces are small, self-limiting and produce minimal symptoms.

Therapeutic drainage of symptomatic pleural effusions

Drainage of large pleural effusions can generally be performed in one step, without leaving an indwelling catheter, provided infection is not present. If a large amount of fluid is to be drained, the aspiration needle is replaced with a catheter to decrease the possibility of trauma to the lung. Short, soft and flexible catheters (7-12 F) may be introduced into the pleural space, using either a trocar or the Seldinger method [(7, 14)]. The use of small indwelling pleural catheters in the management of large plural effusions is a safe, efficacious and cost-effective procedure.

Ultrasound can be used to optimise the position of the drainage catheter (including further manipulation into additional pockets of fluid) and to monitor the amount of fluid remaining.

Catheter drainage of pleural collections

External drainage is a well-accepted treatment option for various types of pleural collections including empyemas, complicated parapneumonic effusions or haemothoraces. The drainage can be performed using either large-bore catheters (>20 F) inserted surgically or small-bore catheters (SBCTs) (<20 F diameter) inserted using ultrasound or CT guidance [(21)]. SBCTs have gained popularity amongst surgeons, respiratory physicians and

oncologists as they are easier to position and typically cause less pain to the patient [(21)]. The success rate of small-bore catheter (10-20 F) drainage is higher for massive transudative effusions (81.6%) and malignant pleural effusions (75.5%), than for parapneumonic effusions/empyemas (72.2%), haemothoraces (66.6%) and pneumothoraces (64.0%) [(21)]. In thoracic empyemas, the success rate ranges between 72-92%, being influenced by the characteristics of the fluid prior to drainage. Thus, in anechoic and complex non-septated collections the success rate is significantly higher (92.3% and 81.5% respectively) than in complex septated collections (success rate of 62.5%) [(22)].

The use of SBCTs has become the standard of care in several clinical conditions such as pneumothoraces, malignant/chronic effusions and simple uncomplicated empyemas. In cases of active, post-traumatic haemothoraces or complicated empyemas, large-bore catheters are still recommended [(21)].

Pleural sclerotherapy

Traditionally, the most common treatment for a persistent, recurrent malignant effusion has been large–bore chest tube (>30 F) drainage followed by instillation of a sclerosing agent (tetracycline, doxycycline, bleomycin, sterile talc) [(23)]. Talc appears to be the most effective and least expensive agent, although there is also evidence for povidone-iodine as an equally efficacious agent [(24)]. Large bore chest tubes, however, limit patient mobility and are uncomfortable.

There is not enough evidence to support the superiority of talc poudrage at thoracoscopy over talc instillation in a suspension form via a chest tube [(24)]. In recent years, the use of tunnelled pleural catheters (TPCs) has increased. A TPC is a silicone tube that is placed into the pleural cavity, tunnelled subcutaneously with a small cuff and the other end exiting the patient with a one-way valve. The system is easily used at home or in an ambulatory setting. There is increasing evidence that TPCs are safe and effective in alleviating symptoms [(24)]. Compared to video-assisted thorascopic talc insufflation, the use of TPCs was associated with a significantly reduced post procedural and overall hospital length of stay and also with significantly fewer ipsilateral reinterventions [(25)].

Ultrasound guidance is used to ensure accurate catheter placement for thoracocentesis and instillation of the chemical agents, to assess adequacy of drainage and re-accumulation of

fluid, to locate loculated fluid collections and to check for re-accumulation of fluid at 24 hours [(7, 23)].

Pneumothorax

The advantages of using thoracic ultrasound for the diagnosis of pneumothorax are striking. It is highly accurate [(26)], extremely quick to perform at the bedside and much more sensitive than physical examination or chest radiography [(27)]. Furthermore, ultrasound is more accurate than supine anterior chest radiography for both ruling out [(28)], [(29)] and ruling in the diagnosis of pneumothorax [(30)].

Sonographic signs of pneumothorax

Ultrasonographic diagnosis of pneumothorax relies on four sonographic signs: the lung sliding, the lung pulse, the B-lines and the lung point [(30, 31)] [Figure 19].

Figure 19 Flow-chart showing the procedure for the sonographic diagnosis of pneumothorax using a combination of the four key signs: lung sliding, B-lines, lung point and lung pulse (adapted from [(32)]).

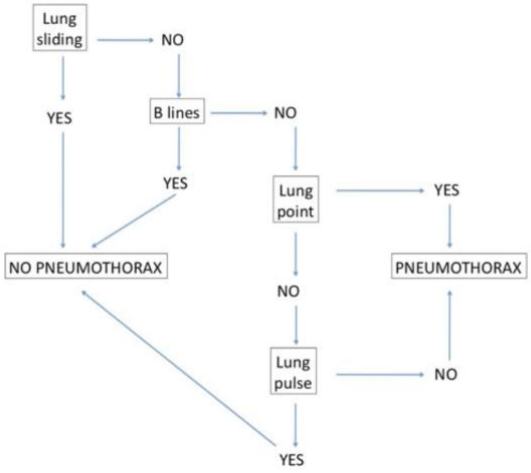

Once the pleural line is visualised as an echogenic horizontal line below the ribs, the first sign to look for is lung sliding, namely, a regular rhythmic, to and fro movement synchronised

with respiration that occurs between the parietal and visceral pleura [(33)]. The lung pulse refers to the subtle rhythmic movement of the visceral pleura upon the parietal pleura that is synchronous with cardiac oscillations [(34)]. The B-lines are discrete, vertical, hyperechoic artefacts, originating from the pleural line and extending to the edge of the screen without fading, moving synchronously with the lung sliding [(35)] [Figure 20].

Figure 20 Lung ultrasound scan showing the pleural line (white arrow). We can also distinguish some vertical, echogenic lines arising from the pleural line that spread up to the edge of the screen without fading: the B-lines (white asterisks).

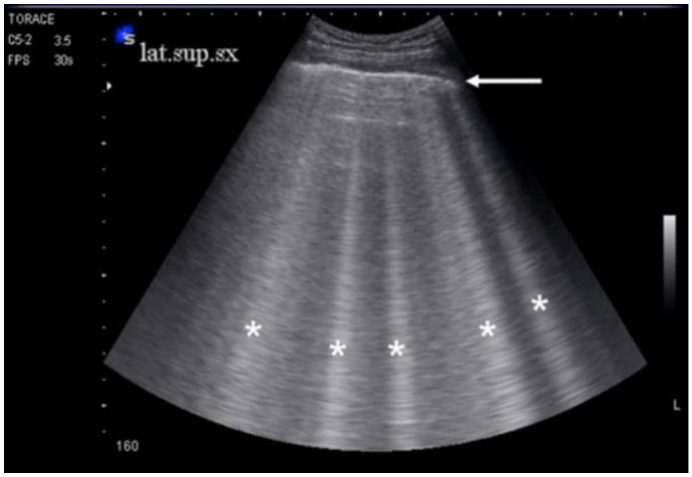

The mere presence of one of those three signs effectively rules out a pneumothorax (at the specific location where the sign is detected). However, their simultaneous absence is not sufficient to make a definitive diagnosis, only to suspect it.

To confirm the diagnosis of a pneumothorax, the fourth sign, the lung point, needs to be visualised. It represents the projection on the chest of the point where the visceral pleura is once again in contact with the parietal pleura without air interposition and sliding reappears after a zone of absence. Therefore, the lung point corresponds to the lateral edge of the pneumothorax in a condition of partial collapse of the lung. Its identification confirms pneumothorax with a positive predictive value of 100% [(36)], however, its sensitivity is low because it is not always easily detectable and in cases of complete lung collapse it cannot be visualised (as there is no point in which the two pleurae get back in touch).

Scanning technique

Sonographic examination to detect a pneumothorax should be performed with the patient in the supine or semi-recumbent position. The scanning technique involves first placing the probe on both sides of the upper chest, where air normally collects for reasons of gravity [Figure 21]. When a sonographic pattern suggestive of pneumothorax is found on the anterior-superior part of the chest (absence of sliding, lung pulse and B-lines), the probe should be moved to the lateral-inferior areas in search of the lung point [Figure 22]. This is the scanning technique recommended for stable patients.

Figure 21 The ultrasound examination for pneumothorax should be performed on a single site on both sides of the upper chest (grey circle), where air collects for reasons of gravity (adapted from [17]).

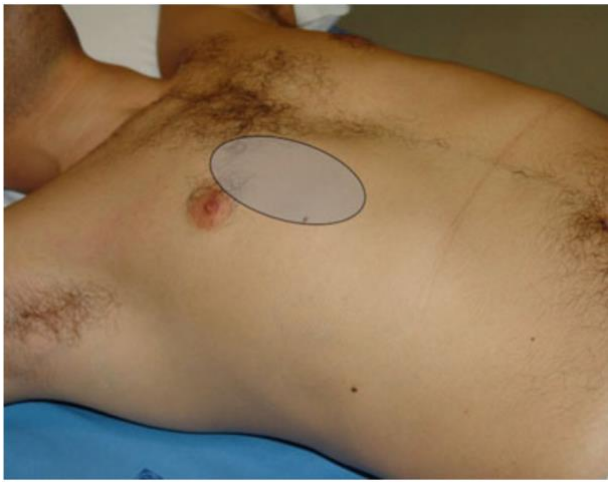

Figure 22 Upper panel: when there is absence of sliding and B-lines in the anterior chest (black crosses), the probe is moved to the lateral areas looking for sudden visualisation of a respiratory pattern (appearance of sliding and B-lines), the lung point (white cross). Lower panel: corresponding CT scan showing right sided pneumothorax. The black arrows show two chest areas where lung sliding cannot be visualised. The white arrow indicates the area where sliding is visualised again, the lung point.

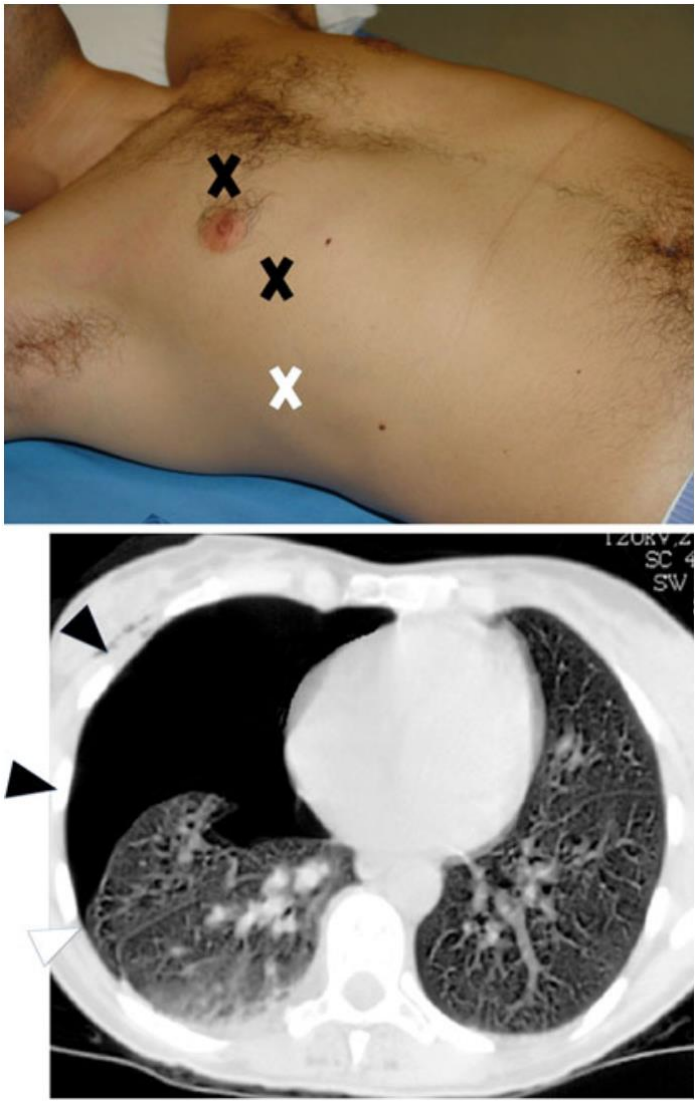

The methodology changes slightly in unstable patients or in the scenario of cardiac arrest. The absence of any sliding, pulse and B-lines bilaterally is enough to confirm the presence of

a pneumothorax and begin treating it. In such cases, there is no need to check for a lung point, because visualisation of this latter sign would not change the decision to drain.

Monitoring pneumothorax size

Thoracic ultrasound can also be used to assess and monitor the size of a pneumothorax. In fact, the projection of the lung point on the chest wall is a sign of the distribution of the air and the laterality of this point is a measure of the superficial extension of the pneumothorax.

It does not directly indicate the volume of the pneumothorax as similar superficial extensions may be observed in different pneumothorax volumes, depending on the distance between the collapsed lung and the chest wall. However, there is good evidence that the position of the lung point allows adequate semi-quantification of the pneumothorax volume in both animals [(37)] and humans [(38)]. A lung point anterior to the mid-axillary line is strongly predictive of lung collapse (and thus of pneumothorax volume) inferior to 15%, while a lung point posterior to that line is strongly predictive of lung collapse greater than 15% with high sensitivity and specificity (83.3% and 82.4% respectively) [(38)].

Consequently, thoracic ultrasound can also be considered a reliable tool to evaluate the residual presence of air in a pneumothorax treated by drainage [(39)]. This evidence demonstrates the potential of ultrasound in monitoring pneumothoraces in many different settings, such as in stable patients to assess treatment success or in trauma patients who require mechanical ventilation, allowing them to be treated in a more conservative way [(40)].

Pitfalls

It is important to be aware that several potential pitfalls may be encountered in the assessment of the lung for the presence or absence a pneumothorax.

Subcutaneous emphysema

The first potential pitfall is the possible presence of non B-line vertical artefacts simulating B-lines and this may happen in the presence of subcutaneous emphysema. In this case, the

vertical artefacts are not arising from the pleural line and are related to the acoustic mismatch between air and liquid, not inside the lung but at the level of the subcutaneous tissues. Therefore, in subcutaneous emphysema, the presence of this type of artefact should corroborate the diagnosis of pneumothorax rather than exclude it (in fact the presence of subcutaneous emphysema is frequently associated with pneumothorax).

Septate pneumothorax

In patients who have a failed pleurodesis after recurrent pneumothoraces it is not uncommon to find a different sonographic pattern in the presence of a pneumothorax. In the same scan, the absence of sliding combined with the persistence of B-lines and lung pulse will be seen. This pattern is related to the presence of lung regions where the parietal and visceral pleura are still in contact due to the presence of septa [(41)]. Demonstrating a lung point in other areas of the chest is a definitive step to confirm the diagnosis of pneumothorax.

Double lung point

When for some reason the air of a pneumothorax is not free to float inside the pleural space, a minimal amount of pleural air may remain in the lateral or dorsal chest. In this case, it is possible to visualise two lung points (the double lung point) which consist of alternating patterns of sliding and non-sliding intermittently appearing at the two opposite sides of the scan. The two lung point represents the visualisation of the two edges of the air trapped within the pleural space [(41)].

Hydropneumothorax

This may be present when an iatrogenic pneumothorax occurs after thoracocentesis. The usual lung point pattern is substituted by an analogous pattern in which an air/fluid interface is present [(42)]. In this case, the lateral edge of the pneumothorax is rendered fluid and called the hydro lung point.

Lung diseases

In healthy people, ultrasound imaging of the lung is not possible because the ultrasound beam is completely reflected at the surface. Pulmonary pathology can be visualised when it extends to the pleura, is accessible via a sound window and no subcutaneous emphysema or pneumothorax is present. Pathology involving only the central parts of the lung? cannot be sonographically visualised and therefore cannot be ruled out with this technique.

Interstitial syndrome

Multiple B-lines are the sonographic sign of lung interstitial syndrome. B-lines are defined as discrete, laser-like, vertical hyperechoic reverberation artefacts that arise from the pleural line (previously described as 'comet tails'), extend to the bottom of the screen without fading and move synchronously with lung sliding. Multiple B-lines are the sonographic sign of lung interstitial syndrome [Figure 20]. Causes of interstitial syndrome include the following conditions:

- Pulmonary oedema of various causes
- Interstitial pneumonia or pneumonitis
- Diffuse parenchymal lung disease (pulmonary fibrosis).

Regarding B-lines, focal multiple B-lines may be present in a normal lung and a focal sonographic pattern of interstitial syndrome may be seen in the presence of pulmonary contusions and pleuritis in particular [(30, 43)].

Pneumonia

In the early congestive stage of pneumonia, the echo texture of the consolidated lung is similar to the liver with aerobilia. However, a marked tree-shaped air bronchogram and a large number of lens shaped echo reflections measuring a few millimetres in size are frequently observed up to the pleura [Figure 23]. In a densely subpleural location, a broad and highly hypoechoic strip, a superficial fluid alveologram, is found. Viral or fungal pneumonias are quite often more poorly ventilated and reveal less marked air bronchograms. Pneumonia is characterised by an irregular, serrated and somewhat blurred

margin. The fluid bronchogram is characterised by anechoic/hypoechoic branched tubular structures in the course of the bronchial tree [(44)]. It does not have a perfusion signal. A persistent fluid bronchogram arouses suspicion of post stenotic pneumonitis and requires suitable bronchoscopic investigation [(45)]. On colour coded duplex sonography, pneumonia has a typical appearance, its circulation is uniformly increased and branched and its vessels have a normal course [(46-49)]. Corresponding to findings seen in colour Doppler sonography, contrast enhanced ultrasound has a short wash-in period and an intensive enhancement [(48)]. The European Federation of Societies for Ultrasound in Medicine and Biology recommends that CEUS is useful and can be applied in differentiating inflammatory from embolic lung consolidation, especially in patients with equivocal CT findings. CEUS may be used in equivocal cases to diagnose lung abscesses within pneumonia, since CEUS appears better than conventional B-mode ultrasound or chest x-ray (CXR) [23]. Bacterial pneumonias tend to fuse and form abscesses which appear as round or oval and largely anechoic foci [Figure 24] [(50)]. Depending on the formation of a capsule, the margin is smooth and echo dense. If a patient does not respond to treatment with antibiotics, the pathogen can be identified by means of ultrasound guided aspiration.

When pneumonia is in the recovery phase, the infiltrated lung tissue is increasingly ventilated. The increase in air gives rise to reflection and reverberation artefacts. The pneumonia recedes on the ultrasound image and appears smaller than on chest radiograph, correlating better to the clinical course [Figure 25].

Table 3 Sonographic findings in pneumonia.

- Liver parenchyma like in the early stage
- Air bronchogram
- Lenticular air trappings
- Fluid bronchogram (poststenotic)
- Blurred and serrated margins
- Reverberation echoes in the margin
- Hypoechoic abscess formation
- Regular vascularisation

Figure 23 Pneumonia in the left upper lung lobe. A large liver-like lung consolidation with marked reflexes of the aerated bronchial tree, the air bronchogram.

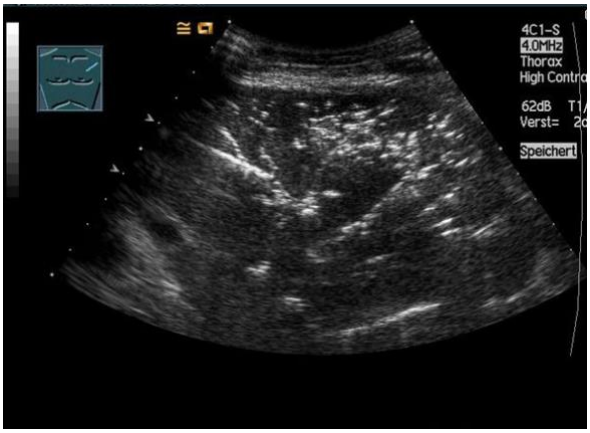

Figure 24 Abscess with persistent fever. Ultrasound guided aspiration surprisingly showed tuberculous bacilli.

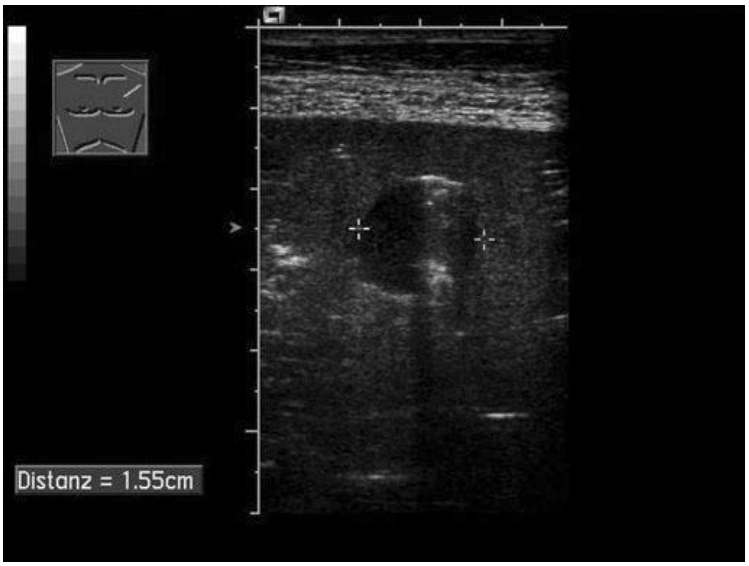

Figure 25 Evolving pneumonia on ultrasound, corresponding to the clinical course. Day 1 (a), Day 5 (b).

a

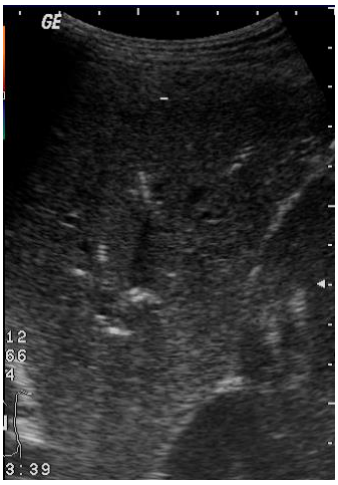

b

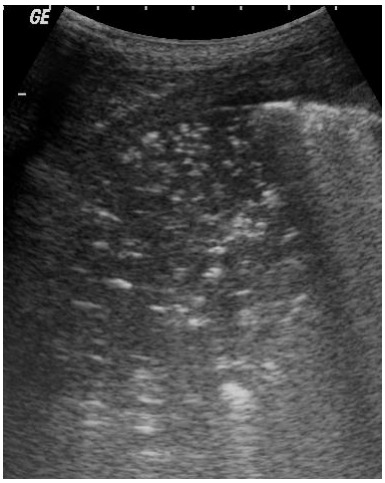

In eight meta-analyses of LUS in community acquired pneumonia (CAP), the overall sensitivity (85-96%) and specificity (80-96%) are very high and its accuracy is more than 90% [Table 4] [42-49]. Therefore, lung ultrasound is able to confirm pneumonia but not to rule it out [43].

Table 4 Data of 8 meta-analyses: LUS in community acquired pneumonia [(51)]

First author	Year	Studies	Pat	Sens	Spec	DOR	AUC	Reference
Chavez MA [42]	2014	12	1353	0.95	0.96	?	0.98	CR/CT
Hu QJ [43]	2014	9	1080	0.97	0.94	510	0.99	CR/CT
Ye X [44]	2014	5	742	0.95	0.90	151	0.97	discharge diag
Berlet T [45]	2015	7	1010	0.91	0.89	?	?	?
Xia Yl [46]	2016	14	1911	0.91	0.90	97	0.97	CT
Llamas AM [47]	2017	16	2359	0.85	0.80	50	0.93	final/discharge
Long L [48]	2017	12	1515	0.88	0.86	65	0.95	CR/CT
Alzahrani S [49]	2017	20	2513	0.85	0.93	174	0.98	clin/imaging

International guidelines recommend CXR as a routine evaluation method for suspected pneumonia. However, CT is now the gold standard for detecting lung consolidation. In six studies that used chest CT as the gold standard, LUS exhibited a pooled sensitivity of 91% and a pooled specificity of 90% [46]. Recent studies show that up to 25% more cases of pneumonia can be visualised on LUS than on CXR when CT is used as the reference method. Thus lung ultrasound will soon replace chest radiography in the diagnosis of acute community-acquired pneumonia.

Tuberculosis

Pulmonary tuberculosis is polymorphic on x-ray as well as on chest sonography. In sonography, tuberculous lung lesions can be round or irregularly shaped and of a relatively homogeneous texture [Figure 26]. The imaging of these lesions may be facilitated by the presence of a pleural effusion. Miliary tuberculosis is characterised by a nodular dissemination of multiple subpleural nodules measuring several millimetres in size. However, the presence of air in the tuberculous cavity may prove artefacts and limit visualisation. The patient's response to tuberculosis treatment can be evaluated by sonography, especially in cases of pleural effusion and subpleural tuberculosis [(48)] [Table 5].

Table 5 Sonographic findings in tuberculosis.

- Pleural effusion
- Fragmentation of visceral pleura
- Subpleural infiltrations of various forms
- Air bronchogram in cases of larger infiltrations
- Broad reflection artefact in cavities

Figure 26 Tuberculosis. Lymphocytic pleural effusion and a subpleural nodule. Diagnosis made by ultrasound guided biopsy.

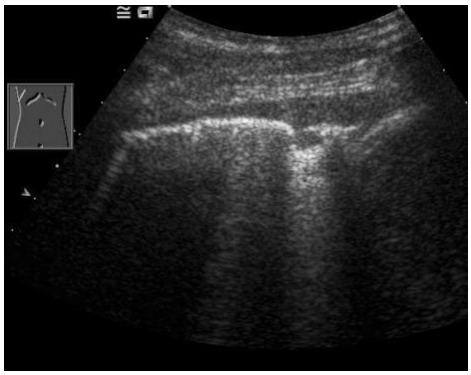

Diffuse parenchymal pulmonary diseases

The ung parenchyma cannot be imaged by sonography. For diffuse parenchymal lung diseases it was shown that multiple ‘comet tail’ artefacts distributed over the entire lung in combination with a thickened, irregular/fragmented pleural line indicate the presence of interstitial changes. In this setting, sonography has almost no value as a primary diagnostic tool. Here, the value of sonography lies in the detection of minimal pleural effusions and subpleural infiltrations in follow up.

Pulmonary embolism

Several minutes after the occlusion of a pulmonary segmental artery, the parenchyma consolidates. Interstitial fluid and erythrocytes flow into the alveolar space. This haemorrhagic congestion offers ideal conditions for ultrasound imaging. These consolidations are open at the periphery along with their base, which creates good conditions for transthoracic sonography. The frequency of haemorrhagic reperfusionable pulmonary infarction is much higher than previously reported, proven by new imaging procedures [Figure 24 and 25]. Sonomorphological criteria of peripheral pulmonary embolism are listed in below [(52-54)] [Table 6].

Table 6 Sonomorphology of peripheral pulmonary embolism [(55)].

- Echo poor
- Well demarcated
- 1-3 (0.5-7) cm in size
- Pleural based
- Triangular > rounded
- Central bronchial reflexion (> 3 cm)
- Vascular occlusion
- 2.5 lesions/patient
- 2/3 located dorsobasally
- Small pleural effusion

In colour Doppler sonography, pulmonary embolism associated subpleural lung consolidations do not show flow signals in the centre of the lesions and the obstruction of blood flow is sometimes at the top of the wedge [(48)]. In contrast agent enhanced ultrasound, very slow and minimal enhancement has been described. Infectious pleuritis or pleuropneumonia can be differentiated by early enhancement and intensive saturation [(49)].

The overall sensitivity of chest sonography in pulmonary embolism is 80% and the specificity is 94% [(55-57)]. In the dynamic process of thromboembolism, chest sonography should be performed in combination with echocardiography and leg vein sonography. With one imaging modality, it is possible to 'kill three birds with one stone': identify the source, "way" and outcome of pulmonary embolism [(55, 57)]. A combination of these three applications enhances the sensitivity of sonography to 92%, an accuracy which cannot be reached with any other imaging modality.

Pulmonary carcinomas and metastases

Lung carcinomas and metastases are sonographically visualised as hypoechoic or moderately echogenic inhomogeneous structures. Mostly they are round, oval or polycyclic. Pulmonary malignancies may have a variable echotexture, sometimes with echo poor necrotic areas [(45, 48)]. They frequently have sharp margins and fringed or finger-shaped striations into the ventilated lung [Table 7, Figure 28].

T-staging

In dynamic ultrasound examination, malignant invasion of the chest wall or subclavian vessels can better depicted by ultrasound than by CT (89%-10% vs 42%-68%). Direct evidence of infiltration of the wall structures and rib destruction are reliable criteria for infiltration of the thoracic wall. An interruption of the pleural reflex and/or limited respiratory motion of the subpleural consolidation provides an indication but not proof of infiltration of the chest wall. Accompanying inflammatory reactions can also cause these signs. Malignant invasion of the chest wall frequently causes local pain. Targeted ultrasound investigation of the region will help to diagnose this condition immediately [(5, 58)].

N-staging

Ultrasound of the supraclavicular and lower cervical lymph nodes has a special role in the staging of bronchial carcinoma since lymph node metastases are identified in 16-26% of all patients. Routine ultrasound evaluation of supraclavicular lymph nodes reveals suspicious

lymph nodes three times more frequently than by palpation and 18%-36% more frequently than CT. Ultrasound guided biopsy can prove malignancy and thereby a N3 or M1 stage [(5)]. In colour Doppler sonography, tumour vessels are irregular and corkscrew like. Reduced vessel visualisation is observed in epidermoid and small cell cancers, supplied by bronchoarterial neovascularisation. Flow signals can be derived from pulmonary arteries in several tumour tissues, particularly in the case of adenocarcinoma and bronchioalveolar carcinomas. Contrast agent enhanced ultrasound shows a delayed start of contrast agent uptake and reduced contrast enhancement. This is an indication of predominant bronchial arterial vascularisation [(59)].

Table 7 Sonomorphology of pulmonary carcinomas

- Hypoechoic, inhomogeneous
- Rounded, polycyclic
- Sharp, serrated margins
- Striations and fringes
- Infiltration of chest wall
- Irregular vascularisation

Figure 27 Lung cancer. Rounded, tumoural fringes, central echo poor necrotic lesion (a) with irregular neovascularisation (b).

a

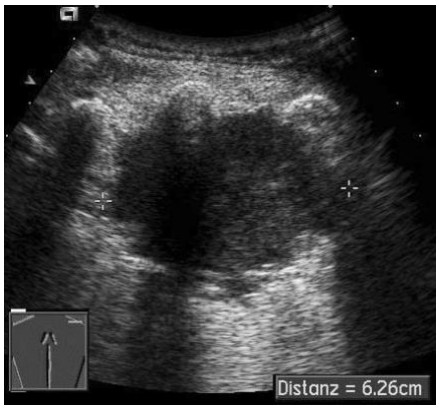

b

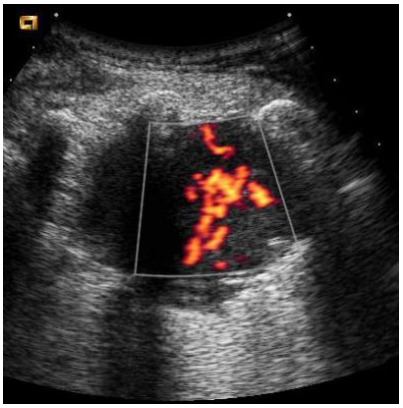

The advantages of ultrasound guided biopsy are many, including rapid availability, low complication rate, the absence of radiation and low cost.

Atelectasis

Lung atelectasis is characterised by the partial or complete absence of ventilation.

Compression atelectasis is caused by large volume pleural effusions. It is largely apneumatic and liver-like. The patient may develop triangular, hypoechoic consolidation shaped like a wedge or a pointed cap and show blurred margins to ventilated lung parenchyma. Compression atelectasis appears to float in the effusion, giving the impression of a waving hand [(45, 48)]. These are partially reventilated during inspiration and after aspiration of the

effusion. In colour Doppler sonography, atelectasis shows increased branch-like vessel visualisation [(49)].

The sonographic image of obstructive atelectasis is marked by a largely homogeneous, hypoechoic presentation of lung tissue in terms of hepatisation. Effusions are absent or small. Depending on the duration of atelectasis, intraparenchymatous structures may also be seen as hypoechoic vascular lines and echogenic bronchial reflexes. Secretory congestion of bronchi presents a fluid bronchogram. The image is similar to that of pneumonia but with significantly less air bronchograms. Obstructive atelectasis has a variable shape. In the case of lobar atelectasis, the border to the ventilated lung is clear and smooth. Sometimes it is also possible to detect an underlying central tumour [(48)]. On colour Doppler sonography, regular vessels are seen along the bronchi. Contrast enhanced ultrasound (CEUS) shows changes that are very similar to pneumonia, but CEUS is seldom necessary [(59)].

In cases of blunt chest trauma, especially if serial rib fractures are present, pulmonary contusions are seen better on sonography than on radiographs. Alveolar oedema and alveolar haemorrhage caused by lung contusions are visualised as hypoechoic, plate-like lesions with partially clear and partially indistinct margins with respect to the ventilated lung [Figure 30]. These are more pronounced in the presence of a concomitant pleural effusion [(60)].

Figure 28 Compression atelectasis: cap-like hypoechoic transformation of lung parenchyma.

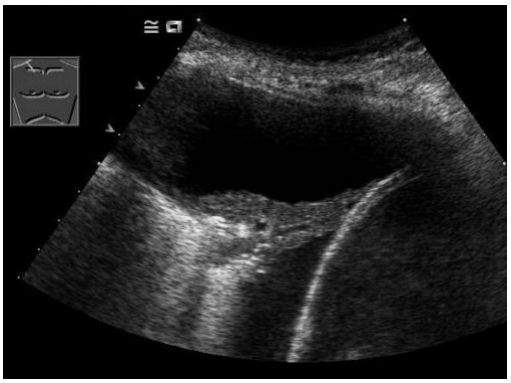

Figure 29 Lung contusion: plate shaped subpleural lung consolidation.

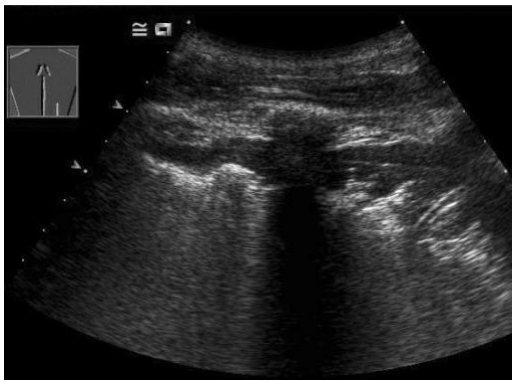

References

1. Mathis G. Thoraxsonography--Part I: Chest wall and pleura. Ultrasound Med Biol 1997;23:1131-1139.
2. Prosch H, Strasser G, Sonka C, Oschatz E, Mashaal S, Mohn-Staudner A, Mostbeck GH. Cervical ultrasound (US) and US-guided lymph node biopsy as a routine procedure for staging of lung cancer. Ultraschall Med 2007;28:598-603.
3. Dubs-Kunz B. Sonography of the chest wall. Eur J Ultrasound 1996;3:103-111.
4. Bitschnau R, Gehmacher O, Kopf A, Scheier M, Mathis G. [Ultrasound diagnosis of rib and sternum fractures]. Ultraschall Med 1997;18:158-161.
5. Prosch H, Mathis G, Mostbeck GH. Percutaneous ultrasound in diagnosis and staging of lung cancer. Ultraschall Med 2008;29:466-478; quiz 479-484.
6. Reuss J. Sonography of the pleura. Ultraschall Med 2010;31:8-22, quiz 23-25.
7. Dietrich CF, Mathis G, Cui XW, Ignee A, Hocke M, Hirche TO. Ultrasound of the pleurae and lungs. Ultrasound Med Biol 2015;41:351-365.
8. Yang PC, Luh KT, Chang DB, Wu HD, Yu CJ, Kuo SH. Value of sonography in determining the nature of pleural effusion: analysis of 320 cases. AJR Am J Roentgenol 1992;159:29-33.
9. Chen HJ, Tu CY, Ling SJ, Chen W, Chiu KL, Hsia TC, Shih CM, et al. Sonographic appearances in transudative pleural effusions: not always an anechoic pattern. Ultrasound Med Biol 2008;34:362-369.
10. Bugalho A, Ferreira D, Dias SS, Schuhmann M, Branco JC, Marques Gomes MJ, Eberhardt R. The diagnostic value of transthoracic ultrasonographic features in predicting malignancy in undiagnosed pleural effusions: a prospective observational study. Respiration 2014;87:270-278.
11. Sartori S, Tombesi P. Emerging roles for transthoracic ultrasonography in pleuropulmonary pathology. World J Radiol 2010;2:83-90.
12. Beckh S, Bolcskei PL, Lessnau KD. Real-time chest ultrasonography: a comprehensive review for the pulmonologist. Chest 2002;122:1759-1773.
13. Almolla J, Balconi G. Interventional ultrasonography of the chest: Techniques and indications. J Ultrasound 2011;14:28-36.

14. Blank W, Heinzmann A: Thoracic interventions. In: Dietrich C, Nuernberg D, eds. Interventional ultrasound; a practical guide and atlas: Georg Thieme Verlag KG, 2015; 260-273.
15. Sconfienza LM, Mauri G, Grossi F, Truini M, Serafini G, Sardanelli F, Murolo C. Pleural and peripheral lung lesions: comparison of US- and CT-guided biopsy. Radiology 2013;266:930-935.
16. Ferreiro L, Suarez-Antelo J, Valdes L. Pleural procedures in the management of malignant effusions. Ann Thorac Med 2017;12:3-10.
17. Cavanna L, Mordenti P, Berte R, Palladino MA, Biasini C, Anselmi E, Seghini P, et al. Ultrasound guidance reduces pneumothorax rate and improves safety of thoracentesis in malignant pleural effusion: report on 445 consecutive patients with advanced cancer. World J Surg Oncol 2014;12:139.
18. Adams RF, Gleeson FV. Percutaneous image-guided cutting-needle biopsy of the pleura in the presence of a suspected malignant effusion. Radiology 2001;219:510-514.
19. Zhang Y, Tang J, Zhou X, Zhou D, Wang J, Tang Q. Ultrasound-guided pleural cutting needle biopsy: accuracy and factors influencing diagnostic yield. J Thorac Dis 2018;10:3244-3252.
20. Adams RF, Gray W, Davies RJ, Gleeson FV. Percutaneous image-guided cutting needle biopsy of the pleura in the diagnosis of malignant mesothelioma. Chest 2001;120:1798-1802.
21. Liu YH, Lin YC, Liang SJ, Tu CY, Chen CH, Chen HJ, Chen W, et al. Ultrasound-guided pigtail catheters for drainage of various pleural diseases. Am J Emerg Med 2010;28:915-921.
22. Shankar S, Gulati M, Kang M, Gupta S, Suri S. Image-guided percutaneous drainage of thoracic empyema: can sonography predict the outcome? Eur Radiol 2000;10:495-499.
23. Klein JS, Schultz S, Heffner JE. Interventional radiology of the chest: image-guided percutaneous drainage of pleural effusions, lung abscess, and pneumothorax. AJR Am J Roentgenol 1995;164:581-588.
24. Desai NR, Lee HJ. Diagnosis and management of malignant pleural effusions: state of the art in 2017. J Thorac Dis 2017;9:S1111-s1122.
25. Hunt BM, Farivar AS, Vallieres E, Louie BE, Aye RW, Flores EE, Gorden JA. Thoracoscopic talc versus tunneled pleural catheters for palliation of malignant pleural effusions. Ann Thorac Surg 2012;94:1053-1057; discussion 1057-1059.
26. Reissig A, Kroegel C. Accuracy of transthoracic sonography in excluding post-interventional pneumothorax and hydropneumothorax. Comparison to chest radiography. Eur J Radiol 2005;53:463-470.
27. Soldati G, Testa A, Sher S, Pignataro G, La Sala M, Silveri NG. Occult traumatic pneumothorax: diagnostic accuracy of lung ultrasonography in the emergency department. Chest 2008;133:204-211.
28. Blaivas M, Lyon M, Duggal S. A prospective comparison of supine chest radiography and bedside ultrasound for the diagnosis of traumatic pneumothorax. Acad Emerg Med 2005;12:844-849.
29. Rowan KR, Kirkpatrick AW, Liu D, Forkheim KE, Mayo JR, Nicolaou S. Traumatic pneumothorax detection with thoracic US: correlation with chest radiography and CT--initial experience. Radiology 2002;225:210-214.
30. Volpicelli G, Elbarbary M, Blaivas M, Lichtenstein DA, Mathis G, Kirkpatrick AW, Melniker L, et al. International evidence-based recommendations for point-of-care lung ultrasound. Intensive Care Med 2012;38:577-591.
31. Lichtenstein DA, Meziere G, Lascols N, Biderman P, Courret JP, Gepner A, Goldstein I, et al. Ultrasound diagnosis of occult pneumothorax. Crit Care Med 2005;33:1231-1238.

32. Volpicelli G. Sonographic diagnosis of pneumothorax. Intensive Care Med 2011;37:224-232.
33. Lichtenstein DA, Menu Y. A bedside ultrasound sign ruling out pneumothorax in the critically ill. Lung sliding. Chest 1995;108:1345-1348.
34. Lichtenstein DA, Lascols N, Prin S, Meziere G. The "lung pulse": an early ultrasound sign of complete atelectasis. Intensive Care Med 2003;29:2187-2192.
35. Lichtenstein D, Meziere G, Biderman P, Gepner A. The comet-tail artifact: an ultrasound sign ruling out pneumothorax. Intensive Care Med 1999;25:383-388.
36. Lichtenstein D, Meziere G, Biderman P, Gepner A. The "lung point": an ultrasound sign specific to pneumothorax. Intensive Care Med 2000;26:1434-1440.
37. Oveland NP, Lossius HM, Wemmelund K, Stokkeland PJ, Knudsen L, Sloth E. Using thoracic ultrasonography to accurately assess pneumothorax progression during positive pressure ventilation: a comparison with CT scanning. Chest 2013;143:415-422.
38. Volpicelli G, Boero E, Sverzellati N, Cardinale L, Busso M, Boccuzzi F, Tullio M, et al. Semi-quantification of pneumothorax volume by lung ultrasound. Intensive Care Med 2014;40:1460-1467.
39. Galbois A, Ait-Oufella H, Baudel JL, Kofman T, Bottero J, Viennot S, Rabate C, et al. Pleural ultrasound compared with chest radiographic detection of pneumothorax resolution after drainage. Chest 2010;138:648-655.
40. Kirkpatrick AW, Rizoli S, Ouellet JF, Roberts DJ, Sirois M, Ball CG, Xiao ZJ, et al. Occult pneumothoraces in critical care: a prospective multicenter randomized controlled trial of pleural drainage for mechanically ventilated trauma patients with occult pneumothoraces. J Trauma Acute Care Surg 2013;74:747-754; discussion 754-745.
41. Volpicelli G, Boero E, Stefanone V, Storti E. Unusual new signs of pneumothorax at lung ultrasound. Crit Ultrasound J 2013;5:10.
42. Volpicelli G, Lamorte A, Tullio M, Boero E, Stefanone V. Worsening dyspnea and cough following thoracentesis. Chest 2013;144:e1-e3.
43. Dietrich CF, Mathis G, Blaivas M, Volpicelli G, Seibel A, Wastl D, Atkinson NS, et al. Lung B-line artefacts and their use. J Thorac Dis 2016;8:1356-1365.
44. Lichtenstein DA, Lascols N, Meziere G, Gepner A. Ultrasound diagnosis of alveolar consolidation in the critically ill. Intensive Care Med 2004;30:276-281.
45. Mathis G. Thoraxsonography--Part II: Peripheral pulmonary consolidation. Ultrasound Med Biol 1997;23:1141-1153.
46. Yang P. Colour Doppler ultrasound of pulmonary consolidation. Eur J Ultrasound 1996;3:169-178.
47. Reissig A, Kroegel C. Sonographic diagnosis and follow-up of pneumonia: a prospective study. Respiration 2007;74:537-547.
48. Mathis G, Beckh S, Görg C: Subpleural Lung Consolidations. In: Mathis G, ed. Chest Sonography. Volume 3rd Edition: Springer Berlin Heidelberg, 2011; 55-114.
49. Gorg C, Bert T. Transcutaneous colour Doppler sonography of lung consolidations: review and pictorial essay. Part 2: colour Doppler sonographic patterns of pulmonary consolidations. Ultraschall Med 2004;25:285-291.
50. Yang PC. Ultrasound-guided transthoracic biopsy of peripheral lung, pleural, and chest-wall lesions. J Thorac Imaging 1997;12:272-284.
51. Mathis G: Pneumonia. In: Laursen B. C, Rahman M. N, Volpicelli G, eds. Thoracic Ultrasound, 2018.
52. Mathis G, Metzler J, Fussenegger D, Sutterlutti G, Feurstein M, Fritzsche H. Sonographic observation of pulmonary infarction and early infarctions by pulmonary embolism. Eur Heart J 1993;14:804-808.
53. Mathis G. Ultrasound diagnosis of pumonary embolism. Eur J Ultrasound 1996.

54. Lechleitner P, Raneburger W, Gamper G, Riedl B, Benedikt E, Theurl A. Lung sonographic findings in patients with suspected pulmonary embolism. Ultraschall Med 1998;19:78-82.
55. Mathis G, Blank W, Reissig A, Lechleitner P, Reuss J, Schuler A, Beckh S. Thoracic ultrasound for diagnosing pulmonary embolism: a prospective multicenter study of 352 patients. Chest 2005;128:1531-1538.
56. Reissig A, Heyne JP, Kroegel C. Sonography of lung and pleura in pulmonary embolism: sonomorphologic characterization and comparison with spiral CT scanning. Chest 2001;120:1977-1983.
57. Niemann E, Egelhof T, Bongratz G. Tranthoracic sonography for detecting pulmonary embolism - a meta analysis Ultraschall in Med 2009;30:150-156.
58. Bandi V, Lunn W, Ernst A, Eberhardt R, Hoffmann H, Herth FJ. Ultrasound vs. CT in detecting chest wall invasion by tumor: a prospective study. Chest 2008;133:881-886.
59. Gorg C. Transcutaneous contrast-enhanced sonography of pleural-based pulmonary lesions. Eur J Radiol 2007;64:213-221.
60. Wustner A, Gehmacher O, Hammerle S, Schenkenbach C, Hafele H, Mathis G. [Ultrasound diagnosis in blunt thoracic trauma]. Ultraschall Med 2005;26:285-290.